

# Location Estimation and Recovery using 5G Positioning: Thwarting GNSS Spoofing Attacks

Aneet Kumar Dutta\*, Sebastian Brandt†, and Mridula Singh‡

CISPA Helmholtz Center for Information Security, Saarbrücken, Germany

## Abstract

The availability of cheap GNSS spoofers can prevent safe navigation and tracking of road users. It can lead to loss of assets, inaccurate fare estimation, enforcing the wrong speed limit, miscalculated toll tax, passengers reaching an incorrect location, etc. The techniques designed to prevent and detect spoofing by using cryptographic solutions or receivers capable of differentiating legitimate and attack signals are insufficient in detecting GNSS spoofing of road users. Recent studies, testbeds, and 3GPP standards are exploring the possibility of hybrid positioning, where GNSS data will be combined with the 5G-NR positioning to increase the security and accuracy of positioning. We design the *Location Estimation and Recovery* (LER) systems to estimate the correct absolute position using the combination of GNSS and 5G positioning with other road users, where a subset of road users can be malicious and collude to prevent spoofing detection. Our *Location Verification Protocol* extends the understanding of Message Time of Arrival Codes (MTAC) to prevent attacks against malicious provers. The novel *Recovery and Meta Protocol* uses road users' dynamic and unpredictable nature to detect GNSS spoofing. This protocol provides fast detection of GNSS spoofing with a very low rate of false positives and can be customized to a large family of settings. Even in a (highly unrealistic) worst-case scenario where each user is malicious with a probability of as large as 0.3, our protocol detects GNSS spoofing with high probability after communication and ranging with at most 20 road users, with a false positive rate close to 0. SUMO simulations for road traffic show that we can detect GNSS spoofing in 2.6 minutes since its start under moderate traffic conditions.

## 1 Introduction

Location information is the most critical and essential for a wide variety of navigation and tracking applications. For ex-

ample, law enforcement officials use ankle bracelets to track the location of an offender on parole [6], logistics and supply chain management companies that handle high-value commodities monitor the locations of every vehicle in their fleet to ensure secure transportation [8, 40], ride-hailing applications use location information for assigning drivers to trips and tracking them for billing [4], and nowadays hardly we can find anyone who is not dependent on Google Maps for navigation. Furthermore, public transport locations are continuously monitored to ensure smooth and timely operation of services [13]. Dependency on location information is further increasing with the development of self-driving vehicles [17].

All the applications stated above use Global Navigation Satellite Systems (GNSS) such as GPS, Galileo, and GLONASS. A GNSS receiver uses the time-of-arrival of the signal from four or more satellites to ascertain its precise location coordinates. It is well known that GNSS is vulnerable to signal spoofing attacks. By using low-cost hardware (<50\$), an external attacker can generate a spoofing signal to change the estimated position at the GNSS receiver [7, 10]. These affordable attack devices can hijack vehicle navigation systems while evading detection by law enforcement [9].

The countermeasures to prevent GNSS spoofing by using cryptographic solutions or leveraging physical-layer signal properties are ineffective in securing vehicular navigation [20, 33, 34]. The recently launched cryptographic authentication techniques like Galileo's Open Service Navigation Message Authentication (OSNMA) [11] authenticates the navigation message contents based on the TESLA protocol [41] and one-way hash functions. Since in GNSS, the user's location is computed based on both the navigation message contents and its time-of-arrival, such localization is still vulnerable to signal relay/replay attacks. Techniques that use physical-layer signal properties are ineffective against strong adversaries capable of completely overshadowing legitimate signals and stealthy attackers, e.g., seamless takeover attacks [45].

On the other hand, 3GPP, the standard organization responsible for developing the 5G New Radio (5G-NR) architecture, is exploring the possibility of hybrid positioning using

\*aneet.dutta@cispa.de

†brandt@cispa.de

‡singh@cispa.de

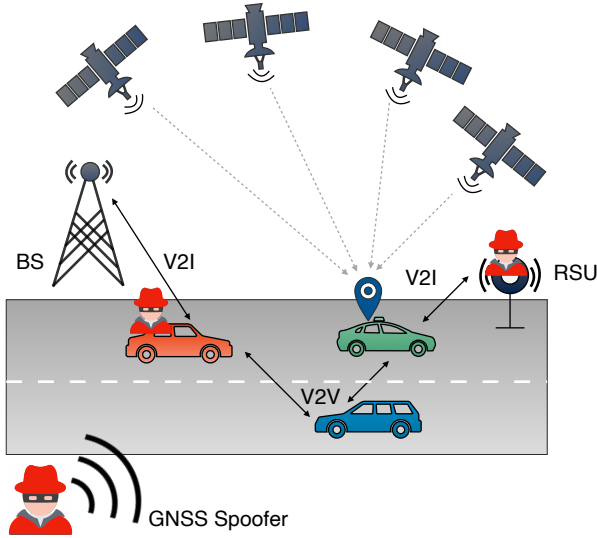


Figure 1: Standards are exploring the possibility of Hybrid positioning by combining GNSS positioning with V2X positioning, which would require ranging of road users with BS, RSUs, and other vehicles. In our design, we consider the presence of GNSS spoofer and road user entities that may collude with the spoofer.

GNSS and 5G-NR. Development of many hybrid positioning testbeds and testing is happening in parallel [3, 12]. The positioning will be enabled using basestations and roadside units, but a strong focus is on enabling vehicle-to-vehicle ranging in order to reduce the load on the infrastructure. While positioning techniques currently added to standards are not designed to provide secure positioning, the research community is actively working to enable secure relative positioning [3, 49].

With this work, we extend the understanding of secure hybrid positioning using the combination of GNSS and 5G. We consider the GNSS spoofing scenario and assume that a subset of the 5G nodes can be malicious (i.e., fake basestation, malicious road users), as illustrated in Figure 1. The goal is to detect and recover from the GNSS spoofing by performing opportunistic distance estimation with other road users and 5G infrastructure. To ensure detection and recovery from the GNSS spoofing, we propose a Location Estimation and Recovery (LER), a hybrid positioning system that combines GNSS and 5G. We make the following contributions:

- We design a Location Verification Protocol to ensure secure distance measurement among road users and with the infrastructure. We extend the concept of Message Time of Arrival Codes (MTACs), a security primitive, to limit spurious distance measurements.
- Our novel recovery and meta-protocol interprets the outcome of distance measurements to detect and recover from the GNSS spoofing while minimizing false alarms.
- We use SUMO simulations to provide optimal time be-

tween the start and detection of the GNSS spoofing.

Using MTACs with multicarrier modulation at the physical layer and trusted components for data processing S-LER protocol limits the distance manipulation caused by malicious users/devices and prevents them from colluding. Analysis using SUMO shows that by using a combination of location verification protocol, recovery and meta protocol, we can detect GNSS spoofing within 2.6 to 4.05 minutes in most traffic conditions, even when each instance of distance measurement is malicious with probability 0.3. These contributions collectively ensure high security guarantees against location manipulation attacks, ensuring safe navigation and tracking of road users.

The remainder of this paper is organized as follows. Sections 2 and 3 provide background and detail the threat model. The LER protocol is explained in Section 4, and analyzed in Section 5. Section 6 complements with further evaluation. We discuss future work in Section 7 and conclude in Section 8

## 2 Background and Related work

### 2.1 GNSS

GNSS is a one-way ranging system. The receivers locate themselves by calculating the time-of-arrival (ToA) of the signals originating from four or more satellites. Due to the availability of cheap software-defined radios, the instances of GNSS spoofing are increasing rapidly. These attacks can be performed by manipulating the data transmitted by the satellites or their arrival time at the receiver [15]. Several countermeasures leveraging spatial diversity, inertial sensors, opportunistic signals, and delayed key disclosure have been studied to increase resilience against GNSS spoofing [44, 47, 52]. The techniques to secure against GNSS spoofing include advanced signal processing [45], Cryptographic method [5, 11], correlating with other sensors, such as inertial navigation system (INS) [39]. With Open Service Navigation Message Authentication (OSNMA), the European Galileo satellite system introduced an anti-spoofing service directly on a civil GNSS signal. Similarly, GPS is expected to use Chips-Message Robust Authentication (Chimera). However, adding authentication does not increase the security of the GNSS, as an adversary can spoof receivers to any location independent of the cryptographic primitive implemented by manipulating the arrival time of the signals [38]. Moreover, even advanced signal processing cannot detect an attacker that completely overshadows the legitimate signal [45]. While attempts have been made to combine inertial navigation sensors and GNSS to detect GNSS spoofing instances in vehicular settings, the build-up of errors in inertial measurement prevents the detection of GNSS spoofing. The existing approaches to detect GNSS spoofing have shortcomings and cannot be trusted to provide secure localization and tracking.

## 2.2 5G Positioning

3GPP standards and 5GAA Automotive Association are exploring the possibility of designing terrestrial positioning infrastructure using 5G-NR [1, 16, 19]. The availability of larger bandwidth makes 5G a perfect fit for high-accuracy positioning. In the transportation sector, road users (cyclists, pedestrians, and vehicles) are expected to use both absolute and relative positioning with assistance from the roadside units (RSU) and base stations (BS). A significant amount of mobility is expected in Cellular Vehicle to Everything (C-V2X) positioning, e.g. vehicle driving by an RSU, a stationary vehicle trying to position with respect to an anchor vehicle that is driving past, etc. These systems are expected to support traffic management and collision prevention. Several field tests are already exploring capabilities of 5G positioning [2, 28].

The 5G standard has currently adopted Observed Time Difference of Arrival (OTDoA) using Positioning Reference Signals (PRS) for distance measurement [31], which are vulnerable to distance manipulation by overshadowing attack [49]. An external adversary can shorten and enlarge the measured distance. Therefore, PRS cannot be trusted to provide secure positioning. The possibility of the two-way ranging is already explored in Release-16. 3GPP has plans to enable secure positioning for C-V2X in Release-18, and it will consider different physical and logical layer designs. The techniques included in the standard so far cannot be trusted to provide secure positioning.

## 2.3 Secure Distance Estimation

The two-way ToF-based ranging systems have emerged as an approach to achieve high precision secure positioning [29, 51]. However, not all ToF-based positioning systems provide secure positioning. The security of wireless positioning depends on logical and physical layer designs and integrity checks at the receiver. Most research on enabling secure positioning focuses on upper bounding measured distance using logical layer cryptographic protocols known as distance bounding protocols [21–25, 27, 32, 46] and then using them for verifiable multilateration [54]. The logical layer distance bounding protocols fall short if an adversary is capable of performing physical layer attacks [30, 36, 42, 43, 50]. An attacker can manipulate distance measurement if the notion of ToA can be manipulated at the receiver. For example, an Early Detect and Late Commit (ED/LC) attacker reduces the measured distance by preemptively injecting a non-committal waveform that triggers an early signal detection [30, 42, 43]. The goal is to cause the receiver to register an earlier ToA, even if the attacker cannot generate the full symbol in advance due to a lack of knowledge about the signal content. An attacker can delay the ToA estimation by overshadowing attacks.

A class of cryptographic primitives, MTACs, have been designed to check the integrity of the ToA manipulation against

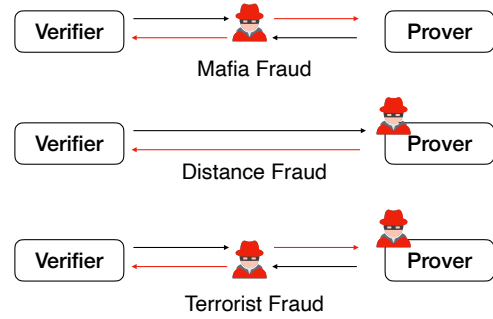


Figure 2: There exists the possibility of different distance manipulation frauds. A malicious user device may exist in the communication region and perform Distance Fraud or use a proxy present in the communication to perform Terrorist Fraud or Distance Hijacking to prove its presence in the communication region.

physical layer attackers. In a similar way that Message Authentication Codes protect message integrity, MTACs preserve the integrity of message arrival times [35]. Existing MTAC designs like V-Range [49] and UWB-ED [48] provide security against distance reduction and enlargement attacks at the physical layer against an external attacker (i.e., Mafia Fraud). Providing security against Mafia Fraud is sufficient for use cases like Passive Keyless Entry and Start systems, where both car and key are part of the same system. However, in collaborative and opportunistic ranging, where the road user (used for the distance estimation) and GNSS spoofer can be the same entity/user, we need to operate under a broader attacker model where the device involved in the distance measurement can be malicious and collude with other attackers.

## 3 Threat Model

First and foremost, we consider the possibility of GNSS spoofing, where an attacker can simultaneously manipulate the GNSS of one or more road users. The attacker may have multiple antennas and perform beamforming to manipulate the perceived location of the receivers to an arbitrary location.

Second, we consider logical and physical layer attacks on the distance the road user measures with other users and infrastructure. We consider the possibility of the external attacker (i.e., Mafia Fraud), where this attacker may want to influence the distance measurement between two legitimate users in order to manipulate the outcome of the hybrid positioning. For these attacks, we consider the possibility of Dolev-Yao’s attacker [26]. Malicious entities can listen to any communication that happen in the communication region, as well as communicate with the other malicious nodes outside the communication region. Within the communication region, they can also inject signals, and through such injection it can block/modify the authentic signals. If successful, this injec-

tion can lead to jamming, signal annihilation, and/or content modification.

We also consider that a malicious entity can be actively involved in distance measurements (i.e., Distance Fraud), such as fake basestations and malicious road users. These attackers can perform GNSS spoofing and distance manipulation simultaneously. While we consider that some of the entities can be owned by an adversary, the application responsible for executing our protocol will run inside a secure integrity-protected processing environment, consisting of memory and storage capabilities [18]. We assume that attacker have limited access to this secure environment. However, the transceiver module used for receiving and transmitting signal for the distance measurement can be a shared resource controlled, as a device many use it for the data communication not related to our application. We also consider that attacker can manipulate internal clock at the receiver in order to manipulate the processing time computed inside the trusted environment.

Moreover, we assume that the malicious users can collude with each other or use legitimate users as a proxy for distance measurement (i.e., Distance Hijacking and Terrorist Fraud).

## 4 Methodology

### 4.1 Overview

We design the Location estimation and Recovery (LER) system, a hybrid positioning system that combines GNSS and 5G positioning to detect spoofing and recover correct location coordinates. The positioning will be mostly carried out between road users using minimal support from the 5G infrastructure. With this protocol, we want to answer the following question: *can we use distance measurements between road users to detect GNSS spoofing? How many such distance measurement instances with other road users will be enough to detect and recover from the GNSS spoofing?*

Since 5G positioning is currently vulnerable to distance manipulation attacks, we cannot directly use them to ensure secure estimation. Therefore, we design a Location Verification Protocol based on V-Range [49]. The V-Range is an MTAC based on Orthogonal Frequency Division Multiplexing (OFDM) and is compatible with the 5G. Since MTAC only provides security against Mafia Fraud, we extended its design to prevent Distance Fraud, Terrorist Fraud, and Distance Hijacking. We use wider subcarrier bandwidth OFDM symbols to reduce the effect of Distance Fraud. The challenge and response for the distance bounding will also be computed inside a trusted environment, and the external part, which may be under the attacker’s control, will not have access to the keys used for computing them. The Location Verification Protocol ensures protection against Mafia Fraud, Distance Hijacking, and Terrorist Fraud and limits the effect of Distance Fraud. Every instance of the Location Verification Protocol between two devices gives a binary output based on whether GNSS

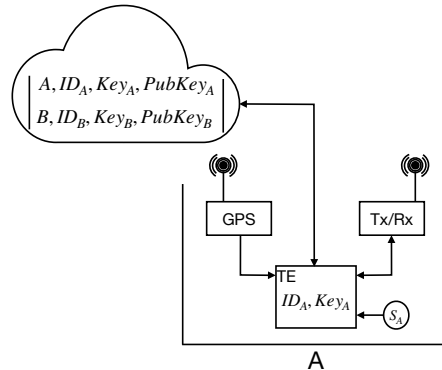


Figure 3: Key distribution, using key server and trusted environment of the user’s device.

coordinates match with distance measurement.

The recovery protocol is the algorithm that interprets the output of the S-LER protocol such that it guarantees GNSS spoofing detection with minimal false positives. The meta-protocol optimizes the parameters for successful GNSS spoofing detection within a fixed number of verification and also minimizes the false positive rate. The algorithm considers the presence of malicious nodes in the verification process and interprets the verification output accordingly. The final weight function obtained captures the temporal and dynamic nature of the mobile entities.

### 4.2 Location Verification Protocol

The Location Verification Protocol enhance MTACs to detect all known distance manipulation attacks by enhancing security at the physical layer as well as on the computation of responses. It is responsible for executing distance bounding with the nearby road users. Each instance of this protocol output the success or failure in matching GNSS coordinates with the distance estimate, which we then feed to Recovery and Meta Protocol to detect and recover from GNSS spoofing. In the following we provide details of the protocol and involved entities.

**Key Server.** It is responsible for providing  $(ID, key)$  pair to all road users. As shown in the Figure 3, we consider that a protocol will be executed between the key server and trusted environment at the user device to obtain a new identity and public key. The device can use the long-term shared key  $(S_k)$  for accessing the server, establishing its identity and obtaining a new pair of  $(ID, key)$ . Assigned  $(ID, Key)$  pair is valid only for the  $T_k$  duration and a new pair is assigned after this time. We also consider that temporary  $(ID, Key)$  pair is only available inside the trusted environment(TE) and it is inaccessible by any unauthorized code or user. We use TE as a concept, where keys will be stored and used for generating challenge and response at the user’s device. We consider TE as the root-of-trust and fully trusted. Also, the adversary

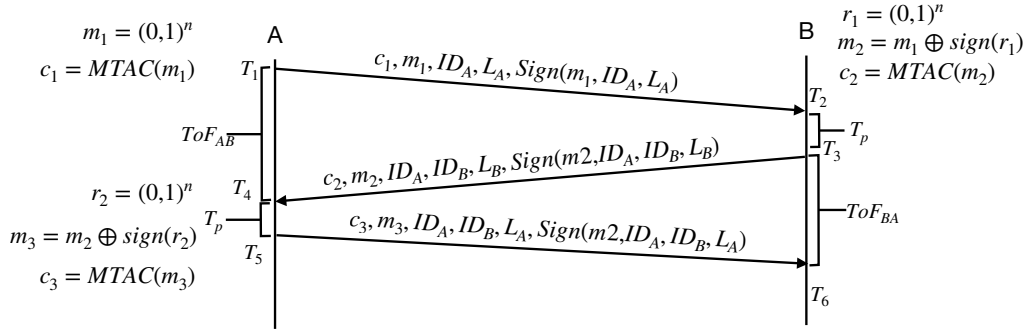


Figure 4: Distance bounding protocol with MTAC.

cannot manipulate  $(Key, ID)$  mapping stored at the server or manipulate it during a query because of the already established public key infrastructure (PKI) in place. However, an adversary can also query the server and acquire the public key  $PubKey$  of any user. One of the important requirements is that each user should be assigned only one ID. Such would be required for many C-V2X applications, where users must rely on other road users for information propagation. We do not provide exact details of the protocol that would be executed between device and key server, as many other applications demand for such architecture. For example, 3GPP is designing the SEAL architecture for key distribution in the C-V2X scenarios [14].

**Verifier and Prover** Any road user, RSU, or BS can assume the role of verifier and prover. The verifier initiates the ranging process with the prover device present in the communication region. The prover responds to the ranging message after processing time  $T_p$ . The verifier and prover can query the key server to access the public key of the prover and verifier, respectively. They both announce their IDs and all the messages transmitted during the protocol execution are tied to them. The integrity of messages can be established by accessing  $PubKey$  associated with these IDs from the key server. In these devices, while time-of-arrival estimation occurs at the transceiver, the received messages are passed to the TE for data-level integrity checks and response computation.

While the Key server is a trusted entity, the verifier and prover can be malicious and collude with the GNSS spoofer. They can share incorrect GNSS coordinates and IDs. For the ranging process, we use a combination of Message Time of Arrival Codes (MTACs) and Digital Signatures (Sign) to check the integrity of arrival time and data, respectively. Each road user can select their role as verifier or prover. We discuss and analyze the security of these design choices in Section 5.

We execute a distance bounding protocol to measure the distance between entities, including road users, RSUs, and BSs. The two entities, A and B, take up the role of the verifier and the prover alternatively. As shown in Figure 5, the following are the protocol steps.

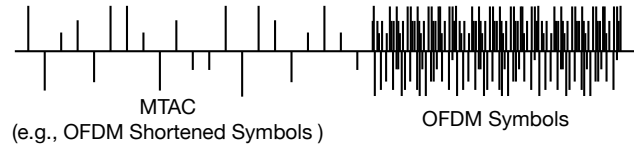


Figure 5: Physical Layer of the messages exchanges for the distance bounding.

1. The entity A takes the verifier role and establishes communication with another entity B. The A transmits the physical layer code  $c_1 = MTAC(m_1)$  at time  $T_1$ , where  $m_1$  is randomly generated by the user A. Along with the code  $c_1$ , the packet sent by the A contains message  $m_1$ , its location coordinates  $L_A, ID_A$ , and the digital signature of this data generated inside TE.
2. The B takes the role of the prover and estimates the arrival time  $T_2$  of  $c_1'$  at the transceiver. The transceiver forwards the code and data to TE for integrity checks and response generation. The B transmits the response after processing time  $T_p$  at time  $T_3$ . The response contain code  $c_2 = MTAC(m_2)$ , location coordinates  $L_B, ID_A, ID_B$ , and digital signature of this data.
3. The A estimate arrival time of code  $c_2'$  as  $T_4$  and forward data to TE for processing. After  $T_p$  duration, at time  $T_5$ , A send an code  $c_3 = MTAC(m_3)$ , its GNSS coordinates  $L_A, ID_A, ID_B$  and digital signature of this data<sup>2</sup>
4. The B estimate arrival time of code  $c_3'$  as  $T_6$ , and forward data to TE for the further processing.
5. In the next iteration, the roles may change between the verifier and the prover.

<sup>1</sup>The received code  $c'$  may not be identical to  $c$  due to channel noise.

<sup>2</sup>The receiver did not need to recalculate the values of  $m_2$  and  $m_3$  as they are directly sent to the receiver and as well as the signed version of message  $m_2$  and  $m_3$  is sent. The receiver retrieves the  $sign(r_i)$  by  $m_1 \oplus m_2$  which will be present to him.

$$\begin{aligned}
 m_2 &= m_1 \oplus sign(r_1) \\
 m_1 \oplus m_2 &= (m_1 \oplus m_1) \oplus sign(r_1) \\
 m_1 \oplus m_2 &= 0 \oplus sign(r_1) \text{ (Since, } A \oplus A = 0) \\
 m_1 \oplus m_2 &= sign(r_1)
 \end{aligned}$$

The message in this protocol contains MTAC, location coordinates, and other information needed for the integrity checks. As shown in Figure 5, shortened OFDM (V-Range) symbols can be used as MTAC, and the remaining data is transmitted as OFDM symbols. After the successful exchange, users can process these messages, even if users  $A$  and  $B$  are no longer in the communication range. In our protocol, it is important to check the integrity of the arrival time of the signal as well as data integrity. The following checks are needed to declare the execution of this protocol successful.

**MTAC Verification.** This check is performed as soon as the signal arrives at the receiver. It is imperative to perform this check for secure time-of-arrival estimation. The exact procedure to perform these checks depends on the MTAC design for transmitting code  $c_i$  [35, 49]. The MTAC verification is done in two steps. First, we must perform a signal integrity check to ensure the code is not maliciously tampered with during the transmission. As shown above, received MTAC samples  $c'_i$  are affected by channel noise and, consequently, are not identical to  $c_i$ . The difference in the  $c_i$  and  $c'_i$  depends on the modulation and channel conditions. Therefore, each receiver may have a different version of the MTAC  $c_i$  due to different channel conditions. The receiver needs to assess the samples' power and variance in  $c'_i$  to perform this check. Once sanity at the physical layer is established, the receiver checks for the bit error. The receiver demodulate code  $c'_i$  to message  $m'_i$  and checks for the bit error by comparing it with the message  $m_i$ . Next, we check for data integrity if signal integrity is established and bit errors are acceptable.

**Data Validation.** Checking the integrity of the messages exchanged between users is crucial. It determines if messages, GNSS coordinates, and ID information exchanged between the users can be trusted. Each user independently queries the key server to acquire public keys of the ID associated with other users. Users  $A$  and  $B$  need access to the public keys of  $B$  and  $A$ , respectively. If the integrity of the messages cannot be established, then the ranging process is marked unsuccessful. This validation ensures that the data is generated within the time  $T_k$  and when location coordinates of entities with  $ID_A$  and  $ID_B$  are  $L_A$  and  $L_B$ , respectively. If multiple ranging are performed with the device with the same ID, then only the first ranging is used, and any further ranging instances are discarded.

**Distance Estimate Validation.** Using GNSS coordinates and estimated arrival time of messages, each user can validate their location coordinates. Using timestamp  $T_1$  and  $T_4$ , the entity  $A$  estimate time-of-flight  $ToF_{AB}$  and compare it with the location coordinates. If  $|(ToF_{AB}/2) - (D_{AB}/c)| \leq \delta$ , where  $D_{AB}$  is the Euclidean distance between the GNSS coordinates of  $A$  and  $B$ ,  $c$  is the speed of signal propagation, and  $\delta$  error allowed in the distance measurement due to channel conditions, then entity  $A$

accept this measurement. Similarly, if  $|ToF_{BA} - (D_{BA}/c)| \leq \delta$ , then entity  $B$  accepts this measurement.

### 4.3 Recovery and Meta Protocol

In this section, we describe the algorithm that uses the output of the verification phase (success/failure) with the neighboring entities to detect GNSS spoofing with minimal false positives in the presence of malicious entities in the network. This algorithm—called the *recovery protocol*—decides when to go into recovery mode based on the information obtained in the verification phase. The two objectives of the recovery protocol are to detect GNSS spoofing as fast as possible when it occurred, and to minimize false positives (i.e., going into recovery mode despite the GNSS not being spoofed). The recovery protocol depends on several parameters that allow the user to fine-tune the protocol to the respective setting (i.e., the assumed percentage of malicious vehicles) and preferences (e.g., the trade-off between speed of spoofing detection and false positives).

To find the optimal parameters in the recovery protocol for any combination of setting and preferences chosen by the user, we provide a meta-protocol for adapting the parameters of the recovery protocol to the chosen setting/preferences (pseudocode in the appendix Section 2). In the meta-protocol, the user can select values for three parameters  $p$ ,  $E$  and  $T$  and is provided with a recovery protocol fine-tuned for this specific parameter combination. The first parameter  $p$  describes the (assumed) percentage of malicious entities in the verification network. The second parameter  $E$  describes the number of distance measurements after which GNSS spoofing is detected in expectation, and the third parameter  $T$  is the number of (most recently) encountered vehicles that the recovery protocol bases its decision on whether to go into recovery mode. In particular, the user can decide how long the protocol is allowed to take to detect GNSS spoofing (which in turn affects the false positives rate)—time here is measured in number of encountered vehicles, but this can be translated to time in seconds via estimations about traffic density. We first describe the recovery protocol and then the meta-protocol for parameter optimization.

#### 4.3.1 The Recovery Protocol

The recovery protocol uses a sliding window mechanism with a sliding window of fixed size  $T$ . The sliding window keeps track of the most recently encountered vehicles; each time a new distance measurement enters the sliding window, the least recently encountered one is dropped from the window, catering to the fact that more recently obtained information is more valuable. Also, each time a new measurement enters the sliding window, a computation takes place based on which the decision is taken whether to go into recovery mode or not. The main two ingredients for this computation are

1. a weight function  $w$  that assigns to each of the  $T$  vehicles in the sliding window an individual weight, where more recently encountered vehicles are given a larger weight (again representing the fact that more recently obtained information is more valuable), and
2. a threshold parameter  $t$  (which represents the trade-off between the speed of spoofing detection and the minimization of false positives).

The first step in the computation is, roughly speaking, to calculate the weighted sum of the failed verification attempts. More precisely, we calculate the sum

$$D = \sum_{i=1}^T (w_i \cdot v_i), \quad (1)$$

where  $w_i$  is the weight assigned to the  $i$ th recently encountered vehicle and  $v_i$  is a binary variable that has value 1 if and only if the coordinates received from the  $i$ th recently encountered vehicle do not match the coordinates provided by the GNSS. In a second step, we compare the obtained sum  $D$  with our threshold parameter  $t$ : if  $D > t$ , then we go into recovery mode, if  $D \leq t$ , then we do not. In the recovery mode, the entity turns to the fully active mode and executes the LER protocol more aggressively. It also increases the frequency of the distance measurement with the RSUs and BSs, as these entities, if available, have a smaller probability of being malicious. By increasing the frequency of protocol execution, the entity forces the attacker to introduce more colluding malicious entities in the communication region.

### 4.3.2 The Meta-Protocol

In this section, we describe how we optimize the parameters for the recovery protocol (in particular, the values of the weight function  $w$  and the threshold value  $t$ ), by means of the meta-protocol. The purpose of the meta-protocol is to obtain a fine-tuned recovery protocol for different settings (characterized by the percentage  $p$  of malicious vehicles) and preferences (characterized by the expected number  $E$  of vehicles after which GNSS spoofing is detected and total window size  $T$ ). Accordingly, the three values  $p$ ,  $E$  and  $T$  are inputs to the meta-protocol, to be specified by the user. As in the recovery protocol, the parameter  $T$  describes the size of the sliding window. Additionally, we will make use of a parameter  $N$  that describes how often certain experiments are repeated in the meta-protocol. Again,  $N$  can be chosen by the user, where higher values for  $N$  provide a better optimization at the expense of an increased runtime of the meta-protocol.

The objective of the meta-protocol is to find a good weight function  $w$  and threshold parameter  $t$  that optimize the recovery protocol for the user-specified values of  $p$ ,  $E$  and  $T$ . Due to the nature of the expression for  $D$  (s. Equation 1) in the recovery protocol (which is clean, but too complex to allow for a direct deduction of the optimal parameters as closed-form expressions), searching for optimal parameters via a

gradient descent approach seems like a good choice. This is supported by the fact that more recently encountered vehicles will be given larger weight in the recovery protocol (providing a monotonic weight function), which makes it plausible that all local minima in the parameter optimization problem are also global minima. Moreover, the experimental results provided in Section 6 confirm that the parameters found by our approach are indeed (close to) optimal. We observe that due to the discrete nature of the recovery protocol, there are entire ranges of parameters (more specifically of the weights of the weight function) that provide exactly the same guarantees, making our optimization task more complicated. We overcome this challenge with an approach based on suitably shrinking intervals.

On a high level, the approach of the meta-protocol is the following: We start with some arbitrary function-threshold pair  $(w, t)$  and then optimize the threshold parameter  $t$  to yield the desired expected number of steps ( $E$ ) for detecting GNSS spoofing when running the recovery protocol with parameters  $w$  and  $t$ . Next, we modify the arbitrarily chosen weight function values index-wise. We increase the weight at a particular index to a much larger value “high” and compute the optimal threshold  $t_{\text{high}}$  and false positives rate  $\text{qual}_{\text{high}}$  of the obtained function. The same procedure is followed by setting the value at the lowest possible value (low = 0) and for a middle value  $\text{mid}$  calculated by  $(\text{low} + \text{high})/2$ . Then we compare the false positive rates  $\text{qual}_{\text{low}}$ ,  $\text{qual}_{\text{mid}}$ , and  $\text{qual}_{\text{high}}$ , and identify intervals of weight values at the chosen index for which the false positives rates are lowest. Then we adjust the high and low values accordingly and repeat this method in a recursive manner until after repeated adjustment of the intervals the interval size becomes very small. The motivation for this approach is to identify the smallest and the largest weight at that particular index that will guarantee to detect GNSS spoofing after  $E$  verifications in expectation and have the lowest false positives rates. Once we identify the smallest and largest for a particular index, the same process is repeated for every other index.

The final  $(w_{\text{opt}}, t_{\text{opt}})$  pair lies within the interval and we always guarantee a monotonic non-increasing weight function to exist. The significance of monotonic non-increasing weight function lies in the fact that the participating entities are dynamic in nature and we are verifying the locations with respect to it. To capture this dynamic and temporal nature of real-world traffic we always choose a monotonic non-increasing function that is guaranteed to lie in the interval which guarantees GNSS spoofing with minimal false positive rate. More precisely, the meta-protocol proceeds as follows (pseudocode in appendix 1).

1. Choose an arbitrary weight function  $w$  and threshold  $t$ .
2. Run the following experiment  $N$  times, each time storing the number of verification steps it takes to go into recovery mode.

- (a) Assume that the GNSS is spoofed and provides false coordinates starting at time 0. Throw a biased coin that shows heads with probability  $1 - p$  for each vehicle encountered after time 0.<sup>3</sup> Whenever we throw heads, the respective vehicle is assumed to be non-malicious, conforming to the expected percentage  $p$  of malicious vehicles.
  - (b) Run the recovery protocol with parameters  $w, t$  on the sequence of vehicles<sup>4</sup> until the protocol decides to go into recovery mode. Here, each non-malicious vehicle  $i$  provides a value of  $v_i = 1$  in the sum (1), while each malicious vehicle  $i$  provides a value of  $v_i = 0$ . This mirrors the fact that the coordinates received from the non-malicious vehicles are exactly those that disagree with the coordinates provided by the (spoofed) GNSS.<sup>5</sup>
3. Compute the average number of verification steps across all  $N$  experiments. If this number is larger than  $E$ , then update  $t$  to a slightly lower value; if it is smaller than  $E$ , then increase it slightly.
  4. Iterate Steps 2 and 3. The updates performed in Step 3 ensure that the pair  $(w, t)$  will get closer and closer to a function-threshold pair that needs exactly  $E$  steps in expectation to reach recovery mode. Consequently, when the average number of verification steps in Step 2 is precisely  $E$ , then we have found the optimal threshold value  $t_{\text{opt}} = t$  for our fixed weight function  $w$ ; in this case terminate the iteration of Steps 2 and 3.
  5. Next, we assign a value  $\text{qual}$  to the obtained pair  $(w, t_{\text{opt}})$  that measures the false positives rate. To this end, we consider the non-spoofed case (in which the coordinates provided by the malicious vehicles disagree with the coordinates provided by the GNSS). For each vehicle in a window of size  $T$ , toss a biased coin that shows heads with probability  $p$  (marking it as a malicious vehicle that will provide a value of  $v_i = 1$  in the recovery protocol), and compute whether the recovery protocol, when executed on this window, would go into recovery mode. Repeat this experiment  $N$  times. The  $\text{qual}$  value for the pair  $(w, t_{\text{opt}})$  is defined as the number of experiments in which the recovery protocol does not go into recovery mode divided by  $N$ , i.e., the fraction of true negatives.
  6. Set the high value to the  $2 \cdot t_{\text{opt}}$  of the first arbitrary function  $w$  chosen and the low value to 0.
7. For each index starting from 0 to  $T$  the following steps are taken with the starting low and high value.
    - (a) Three new weight functions  $w_{\text{low}}$ ,  $w_{\text{mid}}$  and  $w_{\text{high}}$  are obtained, by setting the weight at the chosen index to low, mid, and high, respectively, where  $\text{mid} = (\text{low} + \text{high})/2$ .
    - (b) For each of the three modified weight functions, go to step 2 and obtain the optimal thresholds  $t_{\text{low}}$ ,  $t_{\text{mid}}$ , and  $t_{\text{high}}$ .
    - (c) Now, for the three weight functions and their corresponding optimal thresholds go to 5 and obtain the false positive rates  $\text{qual}_{\text{low}}$ ,  $\text{qual}_{\text{mid}}$  and  $\text{qual}_{\text{high}}$ .
    - (d) Then, based on the false positive rates we obtained, we carry out the recursion in following manner:
      - i. If  $\text{qual}_{\text{mid}}$  is less than  $\text{qual}_{\text{low}}$  set  $\text{low} = \text{low}$  and  $\text{high} = \text{mid}$  and go to step 7a.
      - ii. if  $\text{qual}_{\text{mid}}$  is less than  $\text{qual}_{\text{high}}$  set  $\text{low} = \text{mid}$  and  $\text{high} = \text{high}$  and go to step 7a.
      - iii. Else, we consider the entire interval and split it into two parts i.e.,  $[\text{low}, \text{mid}]$  and  $[\text{mid}, \text{high}]$  and go to 7(d)iiiA for each of the intervals separately.
        - A. If  $\text{qual}_{\text{mid}}$  is less than  $\text{qual}_{\text{high}}$  set  $\text{low} = \text{mid}$  and go to 7(d)iiiA.
        - B. If  $\text{qual}_{\text{mid}}$  is equal to  $\text{qual}_{\text{high}}$  set  $\text{high} = \text{mid}$  and go to 7(d)iiiA.
        - C. if  $\text{qual}_{\text{mid}}$  is higher than  $\text{qual}_{\text{high}}$  set  $\text{mid} = \text{high}$  and go to 7(d)iiiA.
        - D. This will continue until both interval sizes become very small ( $\leq 0.00001$ ). Then we calculate the  $\text{qual}$  value for the four points at the boundaries of the two intervals and return the two (consecutive) points where the  $\text{qual}$  value is highest. These two points will comprise the lower bound and the higher bound for the weight at that particular index.
    - (e) Go to the next index and continue from 7a.
  8. Finally, we make use of the intuition that more recent vehicles should feature with a higher weight in the recovery protocol as follows. Turn the weight function obtained at the end of Step 7a into a monotonically non-increasing function that will lie within the lower and higher bound obtained.

<sup>3</sup>Technically, for each such vehicle, we will only throw the respective coin whenever the vehicle is considered in the subsequent calculations, preventing us from throwing coins prematurely.

<sup>4</sup>This (imaginary) sequence of vehicles is simply characterized by a value for each vehicle that describes whether the vehicle is malicious or not, determined by the respective coin throw.

<sup>5</sup>For malicious vehicles, we can assume in a worst-case fashion that they provide exactly the same coordinates as the spoofed GNSS. This only makes our results stronger as such perfect coordination on the side of the attacker might be hard to achieve.

To briefly illustrate the above protocol, consider the parameter choice  $E = 10$ ,  $T = 30$  and  $p = 0.3$ . Figure 6 shows the lower bound and upper bound for the weights at each index. Figure 6 also demonstrates the monotonic non-increasing weight function that exists within the bounds. The  $\text{qual}$  value achieved in the mentioned setting is 0.9927. The optimal threshold for the mentioned setting is 47.9375.

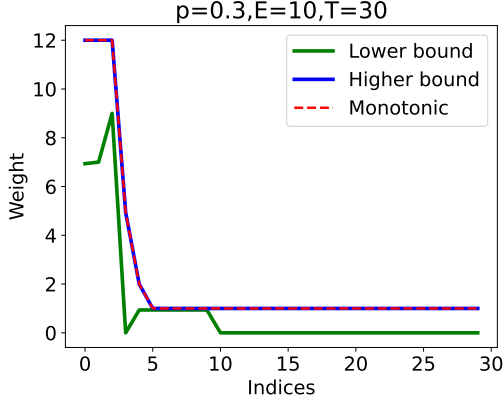


Figure 6: Optimized weight function achieved after executing the meta-protocol

## 5 Security Analysis of Location Verification Protocol

The verification process uses MTAC for GNSS spoofing detection and recovery. The key server is responsible for providing keys for the verification phase of the MTAC and data exchanged during the protocol. In this section, we analyze this protocol in the presence of an adversary. We assume the attacker can spoof the GNSS of the target device to any location of her choice. We also consider that the attacker may have a subset of vehicles under her control, where she can influence the distance measurement. An attacker would manipulate messages or their arrival time to perform attacks. There could be the following attack scenarios for location spoofing: the attacker starts with the cold start, where the attacker manipulates GNSS coordinates when the device is static so that it already has the wrong GNSS coordinates when it starts moving. Otherwise, she starts GNSS spoofing when the entity is already moving on the road and already has some confidence in its location.

The road users continuously measure distance with the nearby node and determine if this distance measurement matches the GNSS coordinates. Therefore, an attacker must pass these checks numerous times to perform a successful GNSS spoofing attack. An attacker cannot use a single malicious node to perform the attack repeatedly. If a node uses the same ID and key mapping for performing ranging in the duration  $T_k$ , then only the first instance of the ranging is considered. In the time duration  $T_k$ , during which the  $ID, key$  pair stays the same, the receiver only considers these nodes once, and they will be again accepted after time duration  $T_k$ . Therefore, selecting the same node again does not help the attacker. Therefore, the attacker needs to either influence the distance measurement between legitimate nodes (i.e., Mafia Fraud) or increase the number of malicious nodes (i.e., Distance Fraud), or collude with the entities outside the communication range

(i.e., Terrorist Fraud). In the following, we analyze the security of the location verification protocol under different distance measurement frauds. While these frauds are mostly named in the literature in regard to the upper bound of the measured distance, we are considering them for both the upper and lower bound of the measured distance

**Mafia Fraud.** Location verification protocol protects against logical and physical layer attacks against an external adversary. For the distance measurement, we use freshly generated nonces and transmit them as MTACs at the physical layer. MTACs, such as V-Range, provide security against distance reduction and enlargement attacks. As shown in Figure 5, if the receiver uses the first part where MTAC is transmitted for the ToA estimation and the remaining part of the signal to validate the data, then the attacker would need to manipulate MTAC during transmission. The physical layer attacks, such as ED/LC, Cicada, signal annihilation, and Overshadowing to advance or delay the signal's arrival time has success probability below  $10^{-4}$  [49].

**Distance Fraud.** We consider that an attacker owns/colludes with a subset of entities. A malicious node in the communication range can transmit incorrect GNSS coordinates as well as compromise any distance measured with this nodes. GNSS coordinates can always be manipulated by spoofing, and distance measured with other entities can be enlarged, for example, by adding a delay circuit between the transmitter and the antenna. Since the legitimate signal has not yet left the device, signal annihilation or overshadowing would not be required.

The possibility of distance shortening by distance fraud depends on the architecture. Suppose the transceiver is a trusted peripheral, accessible only to the trusted environment. In that case, an attacker cannot advance the arrival time of the message, as it would need to advance the arrival time of the message, as in the Mafia Fraud. The stronger possibility is that transceivers would be a shared resource, as the same hardware could be used for the ranging and positioning in 5G [53]. This scenario allows for the distance-shortening attack by distance fraud. For example, an attacker can predict some of the bits of the packet and forward it to the trusted environment for processing, advancing the generation of the response.

Attack success depends on the number of bits an attacker want to predict and the symbol duration. As shown in Figure 7, MTAC and data modulated on the OFDM symbols are needed to produce the correct response. Suppose the receiver has received the whole message except for the last OFDM symbol. In order to advance the arrival time by the OFDM symbol duration  $T_{Sym}$ , the adversary needs to predict data bits modulated on this symbol. Since this symbol carries the digital signature of the freshly generated nonce, an attacker would need to guess the bits. For the OFDM symbols with more than 4000 subcarriers, and 16-QAM modulation, it would be around

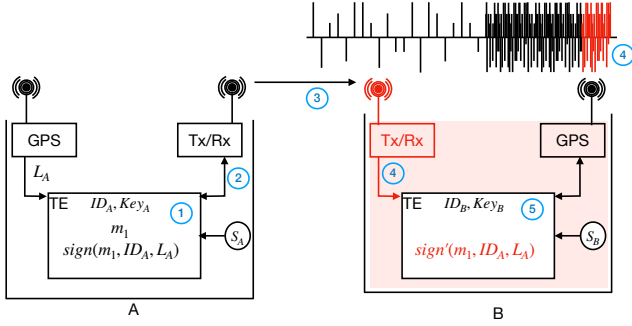


Figure 7: TE and Fraud relation.

guessing 16000 bits. Therefore, an attacker would resort to ED/LC attack. It is shown that the multicarrier time-of-flight ranging is also vulnerable to ED/LC attack. However, the attacker would need  $n_s/4 + 1$  subcarriers for early detection, where  $n_s$  is the number of subcarriers of the OFDM symbols and symbols are 4-QAM or 16-QAM modulated [37]. If we consider processing time zero (processing time will depend on the attacker’s capabilities, but it would be non-zero), the maximum time advancement attacker can achieve is  $3/4$  of the symbol duration. If we use subcarrier spacing of 480 kHz ( $T_{sym} = 2.08\mu s$ ), then attacker can achieve maximum distance shortening of  $\approx 200m$

The trusted environment does not have a trusted local clock. Therefore, an attacker can also manipulate the processing time. Instead of transmitting the response exactly after  $T_p$  time since the arrival of the challenge, an attacker can send it after  $T_p \pm \theta$  time duration. Given that the  $T_p$  is in the order of nanoseconds to a few  $\mu s$ , the maximum error occurring due to this reason would still be limited to a few hundred  $ns$ .

This analysis shows that there are many ways an attacker can manipulate arrival time or the processing time as malicious prover, therefore, we consider that distance reduction and enlargement attacks are possible up to a certain extent due to Distance Fraud. However, it is upper bounded by the duration of the symbol  $T_{sym}$  and processing time  $T_p$ . Therefore, the attacker still needed to be co-located to perform these attacks and cannot perform them if it is remotely located.

**Terrorist Fraud.** In a Terrorist Fraud attack, an attacker close to the Verifier tries to impersonate the prover. In our scenario, this would mean that a malicious entity in the communication region colludes with an entity outside of the communication region. The assumption in terrorist fraud is that prover outside communication regions share short-term keys but do not want to share their long-term secret. Since revealing their long-term secret can lead to impersonation by other malicious entities.

Since our protocol’s security depends on the entities’ diversity that would meet the legitimate entity and help in realizing the GNSS spoofing detection, it is important to prevent this attack. As shown the Figure 7, our challenge and response are

generated inside the trusted environment. While a long-term secret exists outside the trusted environment, the temporary  $(ID, Key)$  is available only inside the trusted environment. This application is also responsible for generating nonces and digital signatures sent as part of the protocol. If the application closes, the  $(ID, Key)$  pair is destroyed. The key required for digital signatures never leaves the trusted environment, so it cannot be shared with other colluders. We consider that Terrorist fraud is not possible without leaking long-term secrets. The sharing of the long-term secret can be further prevented by keeping it in temper-resistant storage.

**Distance Hijacking.** In Distance Hijacking attacks, a dishonest prover convinces the verifier that it is at a different distance than it actually is, by exploiting the presence of an honest prover. For example, one of the ways in which the dishonest prover can achieve this is by hijacking the distance measurement phase of a distance bounding protocol from an honest entity. In our scenario, that would mean that the attacker forces one of the non-malicious entities which are present near the target entity to perform the exchange of MTAC codes. Conceptually, Distance Hijacking can be placed between Distance Fraud and Terrorist Fraud. Unlike Terrorist Fraud, in which a dishonest prover colludes with another attacker, Distance Hijacking involves a dishonest prover interacting with other honest provers. In our protocol, we perform explicit linking to generate the response ( $m_{i+1} = m_i \oplus sign(r_i)$ ), which ensures that the response from different provers is distinguishable by explicitly including identity information in the response, combined with integrity protection.

**Communication Jamming.** The strength of our protocol design is the density and dynamic nature of the traffic. The more entities encountered in the path increase the confidence in the GNSS location and detect GNSS spoofing. In order to prevent GNSS spoofing detection, an attacker can prevent communication with other entities by jamming signals sent by other entities. In the LER protocol, we consider the frequency at which we meet new entities. The information which is acquired before the  $T_k$  becomes redundant. An attacker can prevent communication with other entities, but that would reduce the entity’s confidence in its location and will enter in the recovery phase.

## 5.1 Attacker Influence

The location estimation using the location coordinates and the distance measurement from the neighboring entities requires solving a quadratic equation to find the point at which these circles intersect formed by each node. A single attacker can send malicious data, introduce delays, and do other forms of data manipulation, but it is a single node in a network, since our LER protocol prevents terrorist fraud by its design.

Figure 8(a) and (b) explains the scenario when one entity

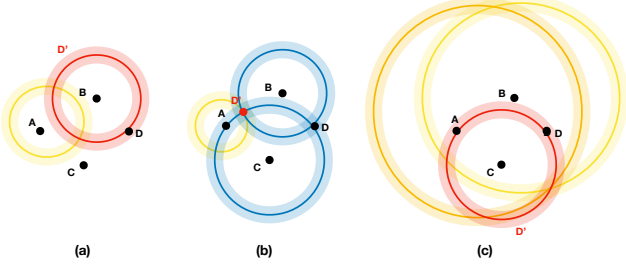


Figure 8: What happens when a subset of active nodes is malicious.

is malicious. The non-malicious entities will share the correct information, and the circles of the respective non-malicious entities will intersect at most two points. In order to spoof the location, the malicious node will have only one choice other than the correct location to spoof. Therefore, even if a malicious entity is active, the scope of the attacker is limited to spoofing to a single incorrect location.

Figure 8(c) explains the scenario when two of three entities are malicious. The non-malicious entities will share the correct information. For successful spoofing to an incorrect location, the malicious nodes will have a choice of anywhere in the circumference of the circle of the non-malicious entity. The choice of attack space increases with the number of malicious entities. For  $n$  active entities of which  $k$  are malicious nodes, successful spoofing is possible only when  $n < 2k + 3$ . The two circles can, at maximum, have two intersecting points. If two active nodes are non-malicious, the third malicious entity only has one choice for a successful attack.

This shows the limitations on the attacker to spoof the location of any entity to any arbitrary location. Also, in order to spoof or fail the verification of any entity, attacker needs to know or preemptively guess the location of the other honest neighboring entities with whom the verification will be done to decide what wrong location it should broadcast and how much distance manipulation it should perform to satisfy the necessary conditions for accepting their wrong location to be a valid one. Also, even if the attacker can figure out the location and the distance manipulation necessary by guessing the neighboring entities (possible in case of less traffic situation) but due to the security guarantee of the LER protocol the attacker might not be able to perform the distance manipulation required. Therefore, in the dynamic setting of vehicular network with continuous secure location verification protocol in place, the chance of success of the attacker is limited. Also, since our protocol prevents terrorist fraud attack the attackers can not collude among each other to fakely increase their presence in the network. Therefore, the number of malicious nodes in the network that will enable failed verification of legitimate GNSS location will be very less.

## 6 Evaluation of the Recovery Protocol

In this section, we evaluate the performance of the recovery protocol described in Section 4.3.1. The design of the recovery protocol ensures that the expected number of verification steps until GPS spoofing is detected does not exceed the value  $E$  selected by the user. In other words, the guarantee that the recovery protocol satisfies in the case that the GPS is spoofed is fully specified by the user. Therefore, the natural way to evaluate the recovery protocol is to consider its performance in the case that the GPS is not spoofed, which is precisely characterized by the relative number of true negatives, i.e., the fraction of times the recovery protocol is not fooled into mistakenly going into recovery mode by malicious vehicles.

In Figure 9, we see the true negative rate of the recovery protocol plotted against the expected number of verifications (specified by the user) until GNSS spoofing is detected. The figure shows the respective curves for three different scenarios ( $p = 0.2, 0.3, 0.4$ ) depending on the assumed probability  $p$  of a vehicle being malicious (also specified by the user). We see that even for the highly unrealistic scenario of each vehicle being malicious with probability  $p = 0.4$ , we reach a fairly large true negative rate by setting the expected number of verifications until GNSS spoofing is detected to a small 2-digit number. In the more realistic setting of  $p = 0.2$ , the true negative rate is very close to 1 (meaning that the recovery protocol is almost never mistakenly going into recovery mode) already for very small values of  $E$ . In conclusion, we get almost optimal results already for the scenario of  $p = 0.2$ ; for smaller  $p$  the true negative rate comes even closer to 1.

In Figure 10, we exemplify the performance of the recovery protocol for the scenarios when we optimized our weight functions with respect to a given percentage  $p = 0.2$  of malicious vehicles (with the expected value for detecting GPS spoofing set to  $E = 7$ ). More precisely, the plotted curve describes the fraction of true negatives as a function of the percentage of malicious vehicles. In particular, we consider the recovery protocol obtained from setting  $p$  to 0.2 (in the optimization performed by the meta-protocol) also in scenarios where the percentage of malicious vehicles is not 0.2. Indeed, in the overwhelming majority of realistic scenarios, the percentage of malicious vehicles can be expected to be much less than 0.2. Our results show that even when the recovery protocol is fine-tuned to the value  $p = 0.2$ , its (already quite good) performance (in terms of true negatives) improves further when the actual percentage of malicious nodes is decreased (e.g., from 0.2 to 0.1), i.e., if we go from a rare worst-case scenario to a much more common scenario. The Figure 10 showcases the true negative rates and it is close to 1 when evaluated with  $p \leq 0.2$ . For values of  $p$  larger than 0.2 the true negative rate decreases quickly; however, this is essentially irrelevant in practice as such large percentages of malicious nodes are virtually impossible in the overwhelming majority of use cases.

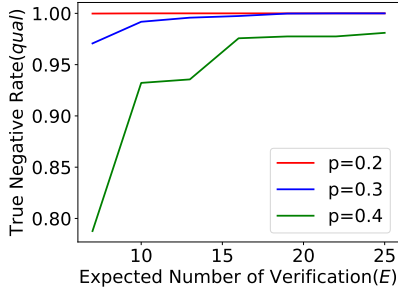


Figure 9: True negative rate achieved for different settings of  $p$  and  $E$ .  $p$  remains same for evaluation & in the meta-protocol.

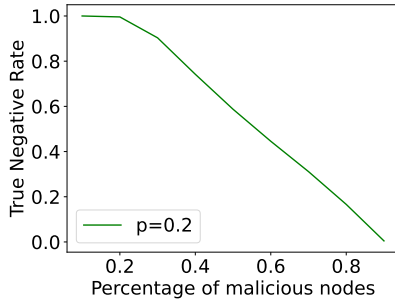


Figure 10: True negative rate for different settings of  $p$  when evaluated for the meta-protocol parameter setting ( $p = 0.2, E = 7, T = 20$ )

While, as explained before, the performance of the recovery protocol is customizable in the case of a spoofed GPS, it is only customizable in terms of the expected value  $E$ ,  $p$  and  $T$ . While an expected value is a perfect indicator for the average number of verification steps until GPS spoofing is detected, sometimes users prefer to have concrete (and small) bounds on the *probability* that the number of steps until spoofing is detected exceeds some desired value. In Figures 11a, 11b and 11c, we plot for each number of verification steps the probability that after this many steps the spoofing has been detected. We provide the evaluation results for the settings given by percentages  $p = 0.05, 0.1, 0.15, 0.2, 0.25, 0.3, 0.35, 0.4$  of malicious vehicles. To evaluate the optimized weight and threshold pair received from the meta-protocol fine-tuned for different sets of parameter  $p = 0.2, 0.3$ , and  $0.4$  and  $T = 20, 30$  and  $50$  respectively. As we can see, even in (fairly unrealistic) scenarios characterized by  $p$ -values that exceed even  $0.2$ , the probability that we have detected GPS spoofing after a reasonably small number of verification steps, e.g.,  $20$  steps, is fairly close to  $1$ . In the much more common scenario of  $p$ -values (far) below  $0.2$ , we detect the GPS spoofing with much smaller number of verifications.

## 6.1 Interpreting the Results using Real-World Traffic Simulation

The proposed protocol is evaluated using Simulation of Urban MObility (SUMO), a traffic simulation package where we

simulated the network of Monaco city<sup>6</sup> and Berlin<sup>7</sup> with the mentioned configuration setting. The simulation results in this section is to showcase how the the numbers provided by the recovery protocol can be interpreted in real-world traffic.

The SuMo simulation for Monaco City is run for a total of 96 minutes and 207 minutes for Berlin. Figure 12 shows us how many number of active vehicles are present in the network at an interval of 1 minute. It also explains how the traffic situation is dynamic in nature and what are the peak traffic time and what is the low or moderate traffic time. The Figure 12 for Monaco shows that initially the number of vehicles inserted in the simulation is less (like early morning/late night traffic in real scenario) and gradually it increases with passing time. The Figure 12 for Berlin demonstrates a completely different traffic pattern from Monaco and thus our protocol is discussed with varying traffic conditions. The simulation data consists of only the neighboring vehicles and not any base stations or RSU information.

In order to utilize the mathematical formulation for GPS detection and recovery, a certain number of vehicles are required. Figure 13 shows the number of unique neighbors the vehicles are encountering with respect to time. The higher the window size  $T$ , the more unique vehicles the entity needs to encounter GNSS spoofing, in turn, higher will be the duration.

Figure 13 demonstrates the time encountered by different entities to meet the required number of vehicles ( $E$ ) to detect GNSS spoofing. Reporting the result of the setting when the percentage of malicious nodes ( $p = 0.2$ ) and the communication range is  $100m$ , the average duration in Monaco is  $2.62$  minutes and for Berlin is  $4.05$  minutes. The simulation results are given in Appendix 14 for the duration with respect to  $T$ .

From the results of the SuMO simulation we can derive the following insights:

- The real-world traffic is dynamic in nature and thus it will be difficult for the attackers to manipulate 20% of the vehicles considering we limit the chance of attacker's success by our secure distance bounding protocol. We have considered,  $p = 0.2$  as a baseline scenario which gives us strong security guarantees and thus, the time estimated in GNSS spoofing detection can be much less in real-world scenario. The unique neighbors encountered does not include the base stations and RSUs, therefore percentage of malicious nodes can also be reduced.
- Based on the traffic scenario and the availability of resources (base-station, RSU), the user can choose its corresponding set of parameters mainly  $p$ . Depending on the  $p$  and  $T$ ,  $E$  will vary. The more the percentage of malicious nodes assumed in the network the higher will be the window size ( $T$ ) and longer will be the duration to detect the spoofing attack.

<sup>6</sup><https://github.com/lcodeca/MoSTScenario>

<sup>7</sup><https://github.com/mosaic-addons/best-scenario>

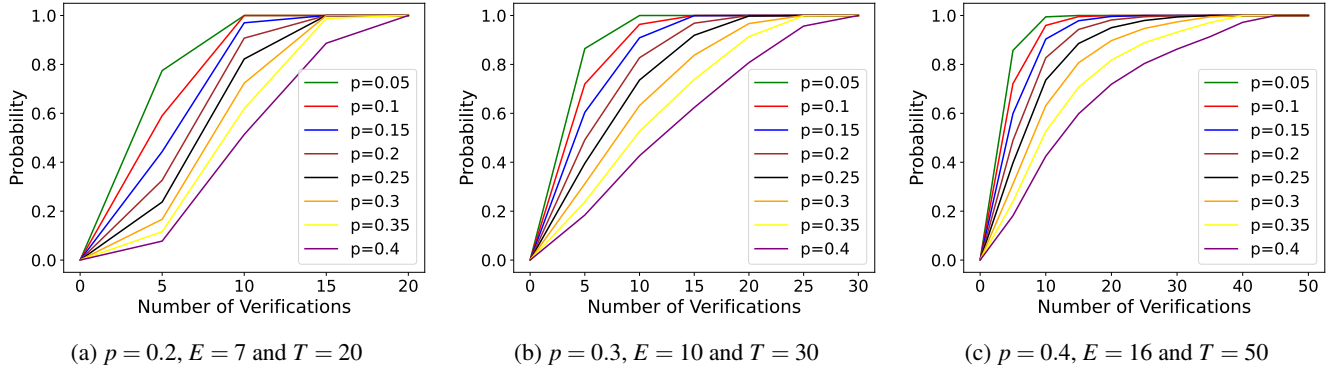


Figure 11: Probability of GPS spoofing detection with respect to the number of verification steps required for different  $p$  settings. The  $p$ -value given in each figure caption indicates the assumed probability *during the execution of the meta-protocol*. The  $p$ -values given in each picture indicate the assumed probability *in the actual setting in which the recovery protocol is applied*.

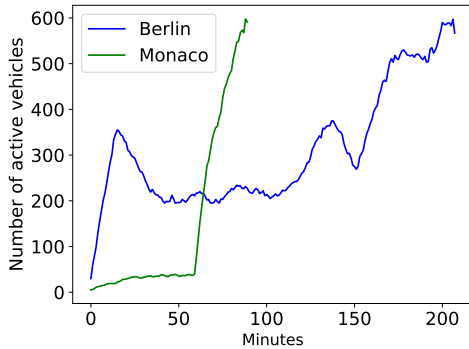


Figure 12: Number of active vehicles in the network in consecutive time periods of 1 minute

## 7 Discussion and Future work

**Device Architecture to prevent Distance Fraud.** Our design takes a step towards using TE to provide security against Terrorist Fraud. However, if the transceiver is malicious, or there does not exist a secure path between the transceiver and TE, then a malicious user can perform distance fraud. Future work should explore the architecture that can overcome this shortcoming of our design by using a secure architecture. If such an architecture can be designed, then the attack would be reduced to distance enlargement by distance fraud, where an attacker can shield the antenna and relay it later, further reducing the effectiveness of the attack.

**Deployment of LER Design.** This protocol can use the transceivers that road users use for communicating with the RSUs and BSs. The protocols need to be run in a secure computing environment. For ride-hailing services, it can be part of the applications. It can be executed inside the ankle bracelet of the offender. For privately owned vehicles, it can be part of the usage-based insurance dongles. In many of these scenarios, the user may not even have root access to the device that performs computation, further reducing the chances of distance fraud.

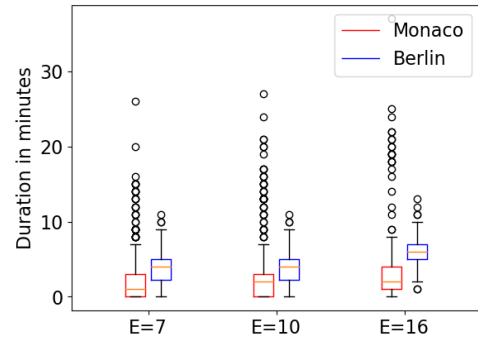


Figure 13: Duration of meeting the expected number of vehicles in different setting when communication range is 100m

**Implementation of TE in LER Design.** In this paper we have proposed the use of TE as a concept for secure distance bounding that provides the root-of-trust in the proposed protocol. The implementation and the performance analysis is still an area to be explored in the context of positioning systems.

## 8 Conclusion

With LER, we propose a protocol to detect GNSS spoofing and recover the correct location coordinates. We used a secure computing environment to prevent remote entities from colluding using Terrorist Fraud. We limited the effect of Distance Fraud by using multi-carrier modulated OFDM Symbols of wider subcarrier bandwidth. We consider the worst-case scenario, where each node is malicious with a probability of 0.3, and show that we can detect it within 2.62 to 4.05 minutes depending upon traffic condition. Using sumo simulations, we confirm that moderate road traffic is sufficient to detect and recover from GNSS spoofing.

## References

- [1] 5G - GPP 38.855 ;Technical Specification Group Radio Access Network; Study on NR positioning support. [https://www.3gpp.org/ftp/Specs/archive/38\\_series/38.855/](https://www.3gpp.org/ftp/Specs/archive/38_series/38.855/). [Online; Accessed 1. November 2022].
- [2] 5GCAR. <https://www.ip45g.de/en/testbeds/5gcar/>. [Online; Accessed 12. April 2023].
- [3] "beyond 5g positioning". <https://research.chalmers.se/en/project/10832>. [Online; Accessed October 10th 2023].
- [4] Car Rental GPS Spoofing. <https://www.carrentalgateway.com/glossary/gps-spoofing/>. [Online; Accessed 12. April 2023].
- [5] CHIMERA GPS. <https://www.gpsexpert.net/chimera-specification>. [Online; Accessed 12. April 2023].
- [6] Crime Prevention System for Public Safety. [https://www.unodc.org/documents/justice-and-prison-reform/ReducingReoffending/MS/Republic\\_of\\_Korea\\_Annex\\_-\\_\\_.pdf](https://www.unodc.org/documents/justice-and-prison-reform/ReducingReoffending/MS/Republic_of_Korea_Annex_-__.pdf). [Online; Accessed 13. April 2023].
- [7] Galileo Open Service Navigation Message Authentication. [https://gssc.esa.int/navipedia/index.php/Galileo\\_Open\\_Service\\_Navigation\\_Message\\_Authentication/](https://gssc.esa.int/navipedia/index.php/Galileo_Open_Service_Navigation_Message_Authentication/). [Online; Accessed 12. April 2023].
- [8] Geotab fleet tracking. <https://www.geotab.com>. [Online; Accessed 13. April 2023].
- [9] "gps spoofing attack sends 38 drivers the wrong way – and into possible danger". <https://shorturl.at/1qt45>. [Online; Accessed October 10th 2023].
- [10] How to Spoof GPS Location with HackRF. <https://drfone.wondershare.com/fake-location/gps-spoofing-with-hackrf-from-windows.html>. [Online; Accessed 18. August 2023].
- [11] OSNMA. <https://shorturl.at/hmuIQ>. [Online; Accessed 12. April 2023].
- [12] Proof of Concept of Hybrid 5G-NR/GNSS Positioning with AD-HOC Overlay. <https://navisp.esa.int/opportunity/details/72/show>. [Online; Accessed 05. July 2021].
- [13] Public Transportation: Bus & Mass Transit GPS. <https://gpstrackit.com/solutions/public-transportation/>. [Online; Accessed 12. April 2023].
- [14] Service Enabler Architecture Layer for Verticals (SEAL); Functional architecture and information flows (3GPP TS 23.434 version 16.4.0 Release 16). [https://www.etsi.org/deliver/etsi\\_ts/123400\\_123499/123434/16.04.00\\_60/ts\\_123434v160400p.pdf](https://www.etsi.org/deliver/etsi_ts/123400_123499/123434/16.04.00_60/ts_123434v160400p.pdf). [Online; Accessed 18. April 2021].
- [15] Spoofing GPS With an SDR. <https://kaitlyn.guru/projects/spoofing-gps-with-an-sdr/>. [Online; Accessed 12. April 2023].
- [16] System Architecture and Solution Development; High-Accuracy Positioning for C-V2X. [https://5gaa.org/content/uploads/2021/02/5GAA\\_A-200118\\_TR\\_V2XHAP.pdf](https://5gaa.org/content/uploads/2021/02/5GAA_A-200118_TR_V2XHAP.pdf). [Online; Accessed 12. April 2023].
- [17] Tesla Hack. <https://www.gpsworld.com/two-years-since-the-tesla-gps-hack>. [Online; Accessed 13. April 2023].
- [18] What is a Trusted Execution Environment (TEE)? <https://www.trustonic.com/technical-articles/what-is-a-trusted-execution-environment-tee/>. [Online; Accessed 18. April 2021].
- [19] 3GPP. [https://www.3gpp.org/ftp/Specs/archive/38\\_series/38.211/](https://www.3gpp.org/ftp/Specs/archive/38_series/38.211/). [Online; Accessed 1. November 2022].
- [20] Dennis M. Akos. Who's afraid of the spoofer? gps/gnss spoofing detection via automatic gain control (agc). *Annual of Navigation*, 59:281–290, 2012.
- [21] Ioana Boureanu, Aikaterini Mitrokotsa, and Serge Vaudenay. Towards Secure Distance Bounding. Cryptology ePrint Archive, Report 2015/208, 2015. <https://eprint.iacr.org/2015/208>.
- [22] Stefan Brands and David Chaum. Distance-bounding protocols. In *EUROCRYPT*, pages 344–359. Springer, 1994.
- [23] Agnès Brelurut, David Gerault, and Pascal Lafourcade. Survey of Distance Bounding Protocols and Threats. In *Foundations and Practice of Security (FPS)*, pages 29 – 49, 2015.
- [24] Čapkun, Srdjan and El Defrawy, Karim and Tsudik, Gene. *Group Distance Bounding Protocols*, pages 302–312. Springer, 2011.
- [25] Cas Cremers, Kasper B. Rasmussen, Benedikt Schmidt, and Srdjan Capkun. Distance hijacking attacks on distance bounding protocols. In *2012 IEEE Symposium on Security and Privacy*, pages 113–127, 2012.
- [26] D. Dolev and A. Yao. On the security of public key protocols. *IEEE Transactions on Information Theory*, 29(2):198–208, 1983.
- [27] Saar Drimer and Steven J. Murdoch. Keep your enemies close: Distance bounding against smartcard relay attacks. In *16th USENIX Security Symposium (USENIX Security 07)*, Boston, MA, August 2007. USENIX Association.
- [28] Hybrid 5G and GPS. [https://www.esa.int/Applications/Navigation/ESA\\_leads\\_drive\\_into\\_our\\_5G\\_positioning\\_future](https://www.esa.int/Applications/Navigation/ESA_leads_drive_into_our_5G_positioning_future). [Online; Accessed June 16, 2020].
- [29] Laura Flueraoru, Silvan Wehrli, Michele Magno, and Dragos Niculescu. On the energy consumption and ranging accuracy of ultra-wideband physical interfaces.

- In *GLOBECOM 2020 - 2020 IEEE Global Communications Conference*, pages 1–7, 2020.
- [30] Manuel Flury, Marcin Poturalski, Panos Papadimitratos, Jean-Pierre Hubaux, and Jean-Yves Le Boudec. Effectiveness of distance-decreasing attacks against impulse radio ranging. In *Proceedings of the Third ACM Conference on Wireless Network Security*, WiSec '10, 2010.
- [31] Mehdi Harounabadi, Dariush Mohammad Soleymani, Shubhangi Bhadauria, Martin Leyh, and Elke Roth-Mandutz. V2x in 3gpp standardization: Nr sidelink in release-16 and beyond. *IEEE Communications Standards Magazine*, 5(1):12–21, 2021.
- [32] Yih-chun Hu, Adrian Perrig, and David Johnson. Ariadne: A secure on-demand routing protocol for ad hoc networks. *Wireless Networks*, 11, 10 2002.
- [33] Todd E. Humphreys. Detection strategy for cryptographic gnss anti-spoofing. *IEEE Transactions on Aerospace and Electronic Systems*, 49(2), 2013.
- [34] Markus Kuhn. An asymmetric security mechanism for navigation signals. volume 3200, 07 2004.
- [35] P. Leu, M. Singh, M. Roeschlin, K. G. Paterson, and S. Čapkun. Message time of arrival codes: A fundamental primitive for secure distance measurement. In *2020 IEEE Symposium on Security and Privacy (SP)*, pages 500–516, 2020.
- [36] Patrick Leu, Giovanni Camurati, Alexander Heinrich, Marc Roeschlin, Claudio Anliker, Matthias Hollick, Srdjan Capkun, and Jiska Classen. Ghost peak: Practical distance reduction attacks against HRP UWB ranging. In *31st USENIX Security Symposium, USENIX Security 2022, Boston, MA, USA, August 10-12, 2022*, 2022.
- [37] Patrick Leu, Martin Kotuliak, Marc Roeschlin, and Srdjan Capkun. Security of multicarrier time-of-flight ranging. In *Annual Computer Security Applications Conference, ACSAC '21*, page 887–899, New York, NY, USA, 2021. Association for Computing Machinery.
- [38] Maryam Motallebighomi, Harshad Sathaye, Mridula Singh, and Aanjhan Ranganathan. Cryptography is not enough: Relay attacks on authenticated gnss signals, 2022.
- [39] Sashank Narain, Aanjhan Ranganathan, and Guevara Noubir. Security of gps/ins based on-road location tracking systems. In *2019 IEEE Symposium on Security and Privacy (SP)*, pages 587–601, 2019.
- [40] Yekutiel A Novik. System and method for fleet tracking. 2000.
- [41] Adrian Perrig, Ran Canetti, J. Doug Tygar, Dawn Xiaodong Song, Leonid Reyzin, and Itsik Mantin. The tesla broadcast authentication protocol. 2002.
- [42] M Poturalski, Mand Flury, P Papadimitratos, JP Hubaux, and JY Le Boudec. The cicada attack: degradation and denial of service in ir ranging. In *Ultra-Wideband (ICUWB), 2010 IEEE International Conference on*, volume 2, pages 1–4. IEEE, 2010.
- [43] Marcin Poturalski, Manuel Flury, Panos Papadimitratos, Jean-Pierre Hubaux, and Jean-Yves Le Boudec. Distance bounding with ieee 802.15.4a: Attacks and countermeasures. *IEEE Transactions on Wireless Communications*, 10(4):1334–1344, 2011.
- [44] M. Rabinowitz, B. W. Parkinson, and J. J. Spilker. Some Capabilities of a Joint GPS-LEO Navigation System. pages 255–265, September 2000.
- [45] Aanjhan Ranganathan, Hildur Ólafsdóttir, and Srdjan Capkun. Spree: A spoofing resistant gps receiver. In *Proceedings of the 22nd Annual International Conference on Mobile Computing and Networking, MobiCom '16*. ACM, 2016.
- [46] Kasper Rasmussen and Srdjan Capkun. Realization of rf distance bounding. pages 389–402, 09 2010.
- [47] Harshad Sathaye, Gerald LaMountain, Pau Closas, and Aanjhan Ranganathan. Semperfi: A spoofer eliminating GPS receiver for uavs. *CoRR*, abs/2105.01860, 2021.
- [48] Mridula Singh, Patrick Leu, AbdelRahman Abdou, and Srdjan Capkun. UWB-ED: Distance enlargement attack detection in Ultra-Wideband. In *28th USENIX Security Symposium (USENIX Security 19)*, pages 73–88, Santa Clara, CA, August 2019. USENIX Association.
- [49] Mridula Singh, Marc Roeschlin, Aanjhan Ranganathan, and Srdjan Capkun. V-range: Enabling secure ranging in 5g wireless networks. In *NDSS 2022*, April 2022.
- [50] Mridula Singh, Marc Roeschlin, Ezzat Zalzal, Patrick Leu, and Srdjan Čapkun. Security analysis of ieee 802.15.4z/hrp uwb time-of-flight distance measurement. In *Proceedings of the 14th ACM Conference on Security and Privacy in Wireless and Mobile Networks*. Association for Computing Machinery, 2021.
- [51] Nils Ole Tippenhauer, Heinrich Luecken, Marc Kuhn, and Srdjan Capkun. Uwb rapid-bit-exchange system for distance bounding. In *Proceedings of the 8th ACM Conference on Security & Privacy in Wireless and Mobile Networks*, WiSec '15, pages 2:1–2:12. ACM, 2015.
- [52] Nils Ole Tippenhauer, Christina Pöpper, Kasper Bonne Rasmussen, and Srdjan Capkun. On the requirements for successful gps spoofing attacks. In *Proceedings of the 18th ACM conference on Computer and communications security*, pages 75–86. ACM, 2011.
- [53] José María Jorquera Valero, Pedro Miguel Sánchez Sánchez, Alexios Lekidis, Pedro Martins, Pedro Diogo, Manuel Gil Pérez, Alberto Huertas Celdrán, and Gregorio Martínez Pérez. *Trusted Execution Environment-Enabled Platform for 5G Security and Privacy Enhancement*, pages 203–223. Springer International Publishing, Cham, 2022.
- [54] S. Čapkun and J. Hubaux. Secure positioning of wireless devices with application to sensor networks. In *IEEE Computer and Communications Societies.*, volume 3, pages 1917–1928, 2005.

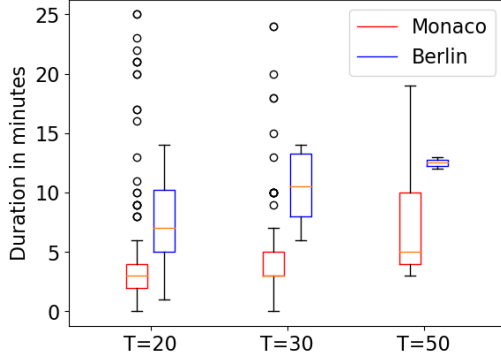


Figure 14: Duration of meeting  $T$  number of vehicles in different setting when communication range is  $100m$

## A Appendix

---

### Algorithm 1: Weight Optimization

---

**Input:** Weight function( $W(i)$ )  
**Output:** ( $W(i)$ ,  $t_{opt}$ ,  $qual$ )  
initialization;  
 $N$  = number of times the experiment is run  
 $T$  = window size;  
 $E$  = Expected number of verification for GPS detection;  
 $t$  = Optimal Threshold( $W(i)$ )  
 $max = 2 - t$   
**for**  $index \leftarrow 0$  **to**  $T$  **do**  
     $value1, value2 = \text{Function1}(W, 0, max)$   
     $lower\_bound_{index} = value1$   
     $higher\_bound_{index} = value2$   
**end**

---



---

### Algorithm 2: Optimal Threshold( $t_{opt}$ )

---

**Input:**  $p$  = percentage of malicious nodes in the network  
Weight function( $W(i)$ )  
**Output:** Optimal Threshold( $t_{opt}$ )  
initialization;  
 $learning\_rate = 1$   
 $flag1 = 0$ ;  
 $flag2 = 0$ ;  
**while** *True* **do**  
     $X = []$ ;  
    **if**  $flag == 1$  &&  $flag2 == 1$  **then**  
         $learning\_rate = learning\_rate / 2$ ;  
    **end**  
    **for**  $i \leftarrow 0$  **to**  $N$  **do**  
         $r = []$ ;  
         $flag = 0$ ;  
        **for**  $j \leftarrow 0$  **to**  $T$  **do**  
             $r.append(\text{flip}(1 - p))$ ;  
             $l = 0$ ;  
             $s = 0$ ;  
            **for**  $k \leftarrow \text{len}(r) - 1$  **to**  $0$  **do**  
                 $s = s + w[l] * r[k]$ ;  
                 $l = l + 1$   
                **if**  $s > t$  &&  $flag == 0$  **then**  
                     $X.append(\text{len}(r))$ ;  
                     $flag = 1$ ;  
                **end**  
            **end**  
        **end**  
    **end**  
     $Y = \sum_{i=1}^N (X)$ ;  
     $L = Y / N$ ;  
    **if**  $L > E$  **then**  
         $t = t - learning\_rate$ ;  
    **end**  
    **else if**  $L < E$  **then**  
         $t = t + learning\_rate$ ;  
    **end**  
    **else**  
         $t_{opt} = t$ ;  
        **return** ( $t_{opt}$ )  
    **end**  
**end**

---



---

### Algorithm 3: Qual Calculation

---

**Input:** Weight function( $W(i)$ ), Optimal threshold( $t_{opt}$ )  
**Output:** True Negative Rate( $qual$ )  
 $count = 0$ ;  
**for**  $i \leftarrow 0$  **to**  $N$  **do**  
     $s = 0$ ;  
     $r = []$ ;  
    **for**  $j \leftarrow 0$  **to**  $T$  **do**  
         $r.append(\text{flip}(p))$ ;  
    **end**  
    **for**  $j \leftarrow 0$  **to**  $T$  **do**  
         $s = s + r[k] * w_0[k]$   
    **end**  
    **if**  $s < t_{opt}$  **then**  
         $count = count + 1$   
    **end**  
    ;  
**end**  
 $qual = count / N$ ;  
**return** ( $qual$ );

---

---

**Algorithm 4: Function1**

---

**Input:**Weight function( $W(i)$ ), lower index( $low$ ), higher index( $high$ )  
**Output:**( $value1, value2$ )  
 $mid = (low + high)/2$   
 $t_{low} = \text{Optimal Threshold}(W_{index}[low])$   
 $qual_{low} = \text{Optimal Threshold}(W_{index}[low], t_{low})$   
 $t_{mid} = \text{Optimal Threshold}(W_{index}[mid])$   
 $qual_{mid} = \text{Optimal Threshold}(W_{index}[mid], t_{mid})$   
 $t_{high} = \text{Optimal Threshold}(W_{index}[high])$   
 $qual_{high} = \text{Optimal Threshold}(W_{index}[high], t_{high})$   
**if**  $qual_{mid} < qual_{low}$  **then**  
|  $value1, value2 = \text{Function1}(W(i), low, mid)$   
**end**  
**else if**  $qual_{mid} < qual_{high}$  **then**  
|  $value1, value2 = \text{Function1}(W(i), mid, high)$   
**end**  
**else**  
|  $value1, value2 = \text{Function2}(W(i), low, mid, mid, high)$   
**end**  
**return** ( $value1, value2$ );

---

---

**Algorithm 5: Function2**

---

**Input:**Weight function( $W(i)$ ),  $low, mid1, mid2, high$   
**Output:**( $value1, value2$ )  
**if**  $mid1 - low \leq 0.00001$  **then**  
|  $z = 1$   
**end**  
**if**  $high - mid2 \leq 0.00001 \ \&\& \ mid1 - low \leq 0.00001$  **then**  
| **if**  $qual_{low} < qual_{mid1}$  **then**  
| |  $value1 = mid1$   
| **end**  
| **else**  
| |  $value1 = low$   
| **end**  
| **if**  $qual_{high} < qual_{mid2}$  **then**  
| |  $value2 = mid2$   
| **end**  
| **else**  
| |  $value2 = high$   
| **end**  
| **return** ( $value1, value2$ )  
**end**  
**else**  
**if**  $z == 0$  **then**  
|  $mid_{new} = (low + mid1)/2$   
|  $t_{mid1} = \text{Optimal Threshold}(W_{index}[mid1])$   
|  $qual_{mid1} = \text{Optimal Threshold}(W_{index}[mid1], t_{mid1})$   
|  $t_{mid_{new}} = \text{Optimal Threshold}(W_{index}[mid_{new}])$   
|  $qual_{mid_{new}} = \text{Optimal Threshold}(W_{index}[mid_{new}], t_{mid_{new}})$   
| **if**  $qual_{mid_{new}} < qual_{mid1}$  **then**  
| |  $value1, value2 = \text{Function2}(W(i), mid_{new}, mid1, mid2, high)$   
| | **return** ( $value1, value2$ );  
| **end**  
| **else if**  $qual_{mid_{new}} > qual_{mid1}$  **then**  
| |  $value1, value2 = \text{Function2}(W(i), low, mid_{new}, mid_{new}, mid1)$   
| | **return** ( $value1, value2$ );  
| **end**  
| **else**  
| |  $value1, value2 = \text{Function2}(W(i), low, mid_{new}, mid2, high)$   
| | **return** ( $value1, value2$ );  
| **end**  
**end**  
**else**  
|  $mid_{new} = (mid2 + high)/2$   
|  $t_{mid2} = \text{Optimal Threshold}(W_{index}[mid2])$   
|  $qual_{mid2} = \text{Optimal Threshold}(W_{index}[mid2], t_{mid2})$   
|  $t_{mid_{new}} = \text{Optimal Threshold}(W_{index}[mid_{new}])$   
|  $qual_{mid_{new}} = \text{Optimal Threshold}(W_{index}[mid_{new}], t_{mid_{new}})$   
| **if**  $qual_{mid_{new}} < qual_{mid2}$  **then**  
| |  $value1, value2 = \text{Function2}(W(i), low, mid1, mid2, mid_{new})$   
| | **return** ( $value1, value2$ );  
| **end**  
| **else if**  $qual_{mid_{new}} > qual_{mid2}$  **then**  
| |  $value1, value2 = \text{Function2}(W(i), mid2, mid_{new}, mid_{new}, high)$   
| | **return** ( $value1, value2$ );  
| **end**  
| **else**  
| |  $value1, value2 = \text{Function2}(W(i), low, mid1, mid_{new}, high)$   
| | **return** ( $value1, value2$ );  
| **end**  
**end**  
**end**

---